International Journal of General Medicine

Dovepress
open access to scientific and medical research

Open Access Full Text Article

ORIGINAL RESEARCH

Retrospective Analysis of the Value of Enhanced CT Radiomics Analysis in the Differential Diagnosis Between Pancreatic Cancer and Chronic Pancreatitis

Xi Ma[1,*]
Yu-Rui Wang[2,*]
Li-Yong Zhuo[1]
Xiao-Ping Yin[1]
Jia-Liang Ren[3]
Cai-Ying Li[4]
Li-Hong Xing[1]
Tong-Tong Zheng[4]

[1]CT/MRI Room, Affiliated Hospital of Hebei University, Baoding, Hebei Province, 071000, People's Republic of China; [2]Department of Computed Tomography, Tangshan Gongren Hospital, Tangshan, Hebei Province, 063000, People's Republic of China; [3]GE Healthcare[Shanghai] Co Ltd, Shanghai, 210000, People's Republic of China; [4]Department of Radiology, The Second Hospital of Hebei Medical University, Shijiazhuang, Hebei Province, 050000, People's Republic of China

*These authors contributed equally to this work

Correspondence: Xiao-Ping Yin
CT/MRI Room, Affiliated Hospital of Hebei University, No. 212 Eastern Yuhua Road, Baoding City, Hebei Province, 071000, People's Republic of China
Tel +86 0312-5981699
Email xpydr_sea123@163.com

Cai-Ying Li
Department of Radiology, The Second Hospital of Hebei Medical University, 215 Eastern Heping Road, Shijiazhuang city, Hebei Province, 050000, People's Republic of China
Tel +86 0311-87046901
Email lcy_dr06@126.com

Purpose: To investigate the feasibility of enhanced computed tomography (CT) radiomics analysis to differentiate between pancreatic cancer (PC) and chronic pancreatitis.

Methods and materials: The CT images of 151 PCs and 24 chronic pancreatitis were retrospectively analyzed in the three-dimensional regions of interest on arterial phase (AP) and venous phase (VP) and segmented by MITK software. A multivariable logistic regression model was established based on the selected radiomics features. The radiomics score was calculated, and the nomogram was established. The discrimination of each model was analyzed by the receiver operating characteristic curve (ROC). Decision curve analysis (DCA) was used to evaluate clinical utility. The precision recall curve (PRC) was used to evaluate whether the model is affected by data imbalance. The Delong test was adopted to compare the diagnostic efficiency of each model.

Results: Significant differences were observed in the distribution of gender ($P = 0.034$), carbohydrate antigen 19-9 ($P < 0.001$), and carcinoembryonic antigen ($P < 0.001$) in patients with PC and chronic pancreatitis. The area under the ROC curve (AUC) value of AP multivariate regression model, VP multivariate regression model, AP combined with VP features model (Radiomics), clinical feature model, and radiomics combined with clinical feature model (COMB) was 0.905, 0.941, 0.941, 0.822, and 0.980, respectively. The sensitivity and specificity of the COMB model were 0.947 and 0.917, respectively. The results of DCA showed that the COMB model exhibited net clinical benefits and PRC shows that COMB model have good precision and recall (sensitivity).

Conclusion: The COMB model could be a potential tool to distinguish PC from chronic pancreatitis and aid in clinical decisions.

Keywords: pancreatic cancer, chronic pancreatitis, radiomics, computed tomography, differential diagnosis

Introduction

Pancreatic cancer (PC) is a highly malignant solid tumor with poor blood supply and no envelope arising from the pancreatic duct cells. The lesion is mainly composed of cancer cells, stromal astrocytes, and interstitial fibrosis and accounts for 2% of all cancers and 5% of cancer-related deaths.[1] The rate of 5-year survival is 2%–9%,[2] and is mainly observed in males and older adults; approximately 90% of the newly diagnosed patients are >55 years.[3] PC has an insidious onset and atypical early symptoms and is often manifested as upper abdominal discomfort,

Received: 2 September 2021
Accepted: 13 December 2021
Published: 6 January 2022

back pain, indigestion, or diarrhea. Patients with symptoms, such as loss of appetite and weight loss, are mostly in the middle and late stages of cancer. At present, the current situation of PC treatment is severe.[4] Surgical resection is the only current option for a cure, but only 20% of PCs are surgically resectable at the time of diagnosis.[5] Mass-forming focal pancreatitis (FP) is a specific type of chronic pancreatitis caused by prolonged inflammation, the destruction of the pancreatic parenchyma, and the proliferation of fibrous tissue.[6] In the early stage of the disease, chronic pancreatitis often receives standardized conservative medical treatment. Surgical indications mainly include failure of conservative treatment commonly used in internal medicine, severe diseases, uncontrollable pancreatitis, compression of adjacent tissue structures, moderate and severe obstruction of biliary tract, main pancreatic duct and duodenum, and pancreatic cancer cannot be ruled out. Autoimmune pancreatitis (AIP) is also a specific type of chronic pancreatitis. Type I focal AIP is pathologically characterized by extensive infiltration of lymphoplasma cells, striated fibrosis, and vasculitis obliterans.[7] Thirty percent of AIP can be relieved by itself. Symptomatic patients are recommended to receive hormone induction therapy. The image performances of FP, localized AIP, and PC are similar and difficult to distinguish; the treatment methods and prognosis of FP, AIP and PC are different, the clinical misdiagnosis often leads to unnecessary surgery.[8]

Therefore, improving the differential diagnostic ability of FP can clinically localize AIP and PC. The gold standard for the diagnosis of PC and chronic pancreatitis is histopathology and cytology, but most patients with PC have already lost the opportunity for surgery when discovered. Computed tomography (CT) is a critical examination method for pancreatic diseases, and radiomics analysis of CT is a rising imaging technology. The high-throughput extraction of medical image radiomics features is applied to quantitatively analyze the distribution characteristics of image pixels or voxel gray levels, provide information that is not visible to the naked eye, and reflect the pathological changes of the lesion. In addition, radiomics has been widely utilized in tumor detection, qualitative diagnosis, differential diagnosis, and prognostic analysis.[9,10] Several studies employed radiomics analysis to differentiate solid pseudopapillary neoplasms of the pancreas, neuroendocrine tumors, and PC, while some studies applied radiomics to distinguish pancreatic serous and mucinous cystadenoma and assess the pathological grade of neuroendocrine tumor.[11–14] However, only a few studies focused on the differential diagnosis of PC and chronic pancreatitis. Thus, the present study aimed to explore the feasibility of distinguishing PC and chronic pancreatitis based on radiomics analysis of CT-enhanced images.

Materials and Methods

Subjects

A total of 151 patients with PC and 24 patients with chronic pancreatitis (18 patients with AIP and six cases of mass pancreatitis) who were admitted to the Affiliated Hospital of Hebei University, Tangshan Workers' Hospital, and the Second Hospital of Hebei Medical University from January 2018 to October 2020 were included in this retrospective study. The study was conducted in accordance with the Declaration of Helsinki and approved by the hospital ethics review committee of Affiliated Hospital of Hebei University, Tangshan Workers' Hospital, and the Second Hospital of Hebei Medical University. Written informed consent was obtained from all participants.

Diagnostic Criteria

PC was diagnosed based on the clinical manifestations, laboratory data, the first image examination before any treatment (surgery, radiotherapy, chemotherapy), and pathological characteristics of the patients.

Mass-forming FP was comprehensively diagnosed based on clinical manifestations, laboratory examinations, and the first image examination before any treatment (surgery, radiotherapy, chemotherapy). After conservative treatment, the lesion shrinks; the phenomenon is further confirmed by surgery and pathology (after the first image examination).

AIP: 1) IGg4 positive or antinuclear antibody-positive; 2) The imaging appearance was typical and consistent with AIP.

Inclusion and Exclusion Criteria

The inclusion criteria for PC were that none of the patients had received radiotherapy or chemotherapy before diagnosis or had a history of other malignant tumors. The inclusion criteria for mass-forming FP and AIP were that none of the patients had been treated before the first examination. Exclusion criteria: 1) patients received other treatments (surgery, radiotherapy, and chemotherapy)

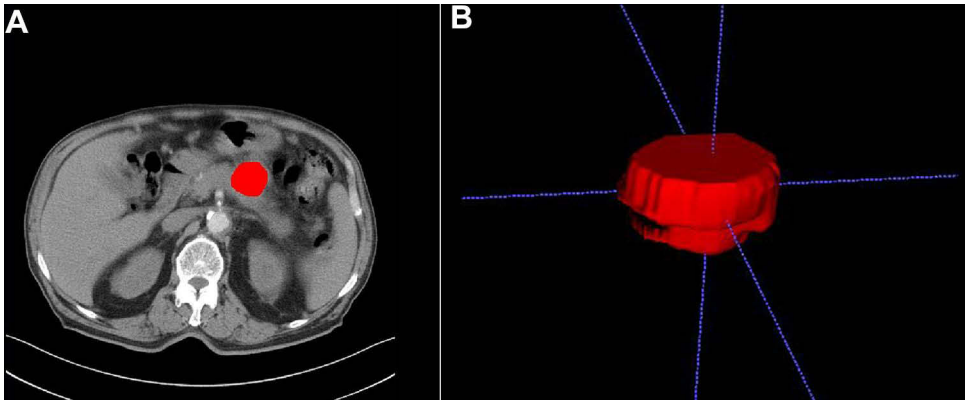

Figure 1 (**A**) ROI of the lesion. (**B**) VOI of the lesion.

before the first scan; 2) artifacts appeared in the image due to patient movement and breathing and were involved in the lesion; 3) CT examination before surgery or treatment was imperfect and lacked complete CT-enhanced image.

Scanning Protocol

Abdominal CT examination of 175 patients was performed using Discovery CT 750 HD (GE Healthcare, Milwaukee, WI, USA), Revolution CT (GE Healthcare), and 64-slice GE Optima CT660 spiral CT (GE Healthcare, Tokyo, Japan). The scanning range was from the hepatic portal to the lower edge of the kidney.

The parameters for Discovery CT 750 HD and Revolution CT were as follows: tube voltage: 120 kV, automatic mA modulation, pitch 0.984, and rack rotation time 0.5 s/cycle. Layer thickness and layer spacing were both 0.625 mm. An EZEM double-barreled high-pressure syringe was used to inject the contrast agent Ioverol (320 mgI/mL) at the flow rate of 3.5 mL/s and dose 1 mL/kg. The start time of the parenchymal phase scan was triggered according to the CT value monitoring of the abdominal aorta at the level of the celiac trunk (Smart Prep Technology). The monitoring threshold was 100 HU. After the threshold was reached, the scan started after a delay of 28 s. The start time of the VP and the balance phase was 30 s and 180 s after the end of the AP.

64-layer GE Optima CT660 spiral CT: tube voltage 80–120 kV, tube current 200–400 mA, pitch 0.984, frame rotation time 0.8 s/cycle, collimator width 0.625×64 mm. A Mallinckrodt double-barreled high-pressure syringe was used to inject the contrast agent Iohexol (320 mgI/mL) at the flow rate of 2.0–3.0 mL/s and dose 0.8–1 mL/kg. The AP and PVP were 30 s, 90 s, and 180 s for delayed scanning.

Image Post-Processing

The images of AP and VP of 151 cases of PC and 24 cases of chronic pancreatitis were imported into MITK software (version: v2021.02, https://www.mitk.org). Two diagnostic physicians with >3 years of work experience independently segmented the lesion and obtained the three-dimensional (3D) volume region of interest (ROI) in all images. The principles of ROI segmentation: 1) delineate layer-by-layer to obtain the ROI volume of the lesion; 2) avoid the blood vessels, pancreaticobiliary duct, and surrounding normal tissues in the lesion; 3) 0–1 mm from the inner side of the edge of the lesion (Figure 1A and B).

Feature Extraction, Selection and Modeling

The DICOM images of AP or VP and the segmentation images are imported into the PyRadiomics toolkit,[15] followed by voxel spacing normalization, Laplacian of Gaussian, and wavelet filtration, and extraction of radiomics features on the original and processed images. Subsequently, a total of 1037 features were obtained in each of the AP and VP, including 18 histogram features, 14 morphological features, 24 gray-level co-occurrence matrices, 16 gray-level run-length matrices, 16 gray-level area matrices, 14 gray-level dependent matrices, and 5 neighbouring gray tone difference matrices. The radiomics feature selection procedure was as follows: 1) preserve features with good consistence; 2) univariate Wilcoxon rank–sum test to retain $P < 0.00005$ (adjusted P value by Bonferroni method) features; 3) correlation analysis to remove the features with correlation >0.9. If two variables have a high correlation, the mean absolute correlation of each variable was obtained and the variable with the largest mean absolute correlation was

removed; 4) the least absolute shrinkage and selection operator algorithm (LASSO) was used to select the most significant features. LASSO is a method of logistic regression analysis that performs feature selection and regularization to improve the prediction accuracy via penalized estimation functions. This maximizes the AUC by tuning parameter (λ) selection and adopts 10-fold cross-validation via minimum criteria. Simultaneously, most covariate coefficients were shrunk to zero and the remaining variables with non-zero coefficients were selected by Lasso. The multivariable logistic regression model was constructed for each phase. Moreover, a radiomics model with the final AP and VP features was established and a clinical feature combined with Radscore, which obtained from radiomics model to construct COMB model. In order to facilitate clinical verification, the nomogram of COMB model was established.

Statistical Analysis

All the statistical analysis was performed using R software (version 3.6.3, https://www.rproject.org). Features with more than 20% missing values are removed, and those with less than 20% are filled with the median value. Reproducibility of radiomics features was assessed with the intraclass correlation coefficient (ICC) and ICC > 0.75 as good consistency. The continuous variables were represented as median (Q1, Q3), and compared using the Wilcoxon rank-sum test. The categorical variables were represented as frequency and compared using the χ^2 test. The discrimination of each model was analyzed by the area under ROC curve (AUC). The Delong test was used to compare the discrimination performances of differential models. The calibration curve and Hosmer–Lemeshow (HL) test was used to evaluate the goodness-of-fit of models. Due to the imbalance of data, the area under the precision recall curve (PRC) is used to further evaluate the effectiveness of the model. Decision curve analysis (DCA) was conducted to evaluate the clinical usefulness by calculating the net benefits at different threshold probability. Two-side $P < 0.05$ was considered statistically significant.

Results

Clinical Characteristics

A total of 151 patients with PC and 24 patients with chronic pancreatitis (18 patients with AIP and six cases of mass pancreatitis) were included in this retrospective study. Statistically significant differences were found in gender, CA19-9, and CEA in patients with PC and chronic pancreatitis between the two groups, but no significant difference was observed in age distribution between the two groups (P > 0.05). Among those with chronic pancreatitis, three patients did not test for CA19-9, and five patients did not test for CEA. Among patients with PC, 13 patients did not test for CA19-9, and 13 did not test for CEA. The clinical demographic characteristics are shown in Table 1.

Model Performance

For AP model, two features of A_original_glszm_SmallAreaLowGrayLevelEmphasis and A_wavelet.LLL_firstorder_10Percentile were reserved. For VP model, two features of V_original_glcm_SumAverage and V_wavelet.LLL_firstorder_10Percentile were selected. After AP and VP features are combined, only VP features are retained after features selection. The final radiomics features are the same as the features of VP model, as shown in the violin chart (Figure 2A). The radscore question as shown in Eq 1. The radscore distribution for each patients is shown in Figure 2B.

Table 1 Comparison of Clinical Data of Patients with Pancreatic Cancer and Chronic Pancreatitis

	Chronic Pancreatitis (N=24)	Pancreatic Cancer (N=151)	*P*-value
Sex			0.034[a]
Male	19 (79.2%)	85 (56.3%)	
Female	5 (20.8%)	66 (43.7%)	
Age	65.000	64.000	0.084[b]
Median (Q1, Q3)	(60.000, 70.000)	(60.000, 70.000)	
CA199 (U/mL)			<0.001[b]
N-Miss	3	13	
Median (Q1, Q3)	498.900 (92.000, 2746.500)	291.600 (46.360, 1982.500)	
CEA (ng/mL)			<0.001[b]
N-Miss	5	13	
Median (Q1, Q3)	7.490 (3.500, 31.975)	6.500 (2.900, 27.070)	

Notes: [a]Pearson's chi-squared test; [b]Wilcoxon rank-sum test.

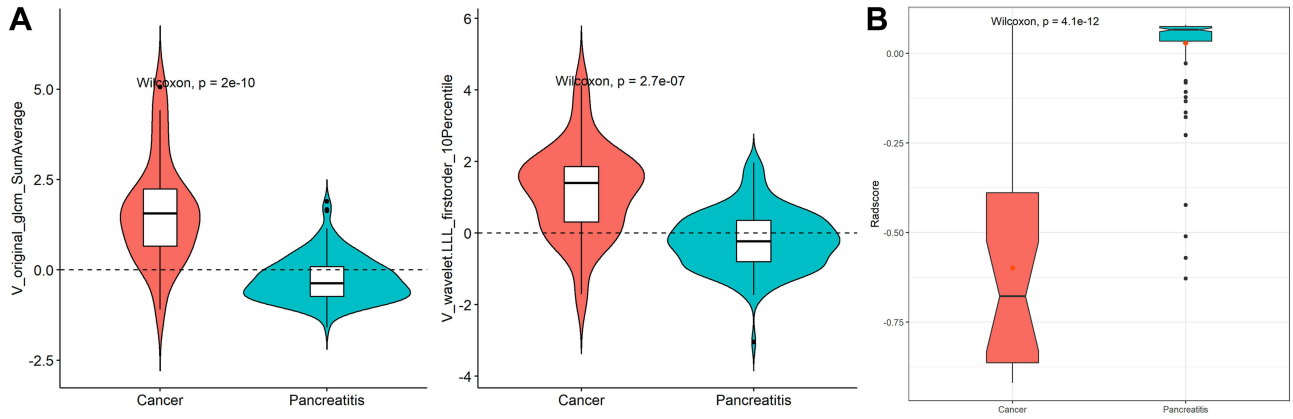

Figure 2 (**A**) Radiomics scores of patients with PC and chronic pancreatitis (Rad-score). (**B**) Numerical values of radiomics characteristics of patients with PC and pancreatitis.

$$radscore = 3.341 - 2.123 \times V_{original_{glcm_{SumAverage}}} - 1.315 \times V\_wavelet.LLL\_firstorder\_10Percentile \quad (1)$$

For the AP model, VP model, radiomics model, clinical model, and COMB model, the AUC values were 0.905 (95% CI: 0.844–0.966), 0.941 (95% CI: 0.860–1.000), 0.941 (95% CI: 0.860–1.000), 0.822 (95% CI: 0.751–0.893), and 0.980 (95% CI: 0.961–1.000), respectively. The more discrimination performance of each model is shown in Table 2 and ROC curve as illustrated in Figure 3.

The results of the Delong test showed that the AUC of the COMB model was significantly higher than that of the AP model (P = 0.004) and Clinical model ($P \leq 0.001$). However, no significant statistical difference was detected between the AUC of COMB model than VP or radiomics models (Table 3).

The calibration curve of each model showed good fitness (Figure 4A) with all HL test $P > 0.05$. The DCA showed that the COMB model had a higher net clinical benefit in threshold range of 0.297–0.883 (Figure 4B). The PRC shows that the COMB model has the highest AUC (0.997) with good precision of 0.96 and recall (sensitivity) of 0.947 (Figure 4C). Then, the COMB model was used to establish a nomogram (Figure 5) for clinical utility.

Discussion

FP, localized AIP, and PC exhibit similar imaging signs, and hence, conventional imaging examination cannot accurately distinguish between these cancers. In recent years, radiomics has developed rapidly, and radiomics analysis has become a hot spot in imaging research. It has been proven that radiomics analysis is useful in distinguishing benign and malignant pancreatic tumors to evaluate the tumor pathological grade and prognosis.[16–18] The accuracy of the radiomics model based on plain CT to identify PC and FP was 93.3%.[19] Zhang et al[20] extracted radiomics features of enhanced CT to distinguish between PC and FP. The results showed that CT images combined with radiomics features improve the diagnostic efficiency significantly. Other studies showed that the diagnostic efficiency of the radiomics model based on PET-CT images to distinguish between PC and AIP is significantly higher than that of the clinical prediction model.[21]

Furthermore, the present study extracted CT-enhanced images of the AP and VP and combined these with clinical

Table 2 Efficacy of Each Differential Diagnosis Model

	AUC	Accuracy	Sensitivity	Specificity
Clinical model	0.822 (0.751–0.893)	0.771 (0.702–0.831)	0.762 (0.505–0.835)	0.833 (0.583–0.958)
AP model	0.905 (0.844–0.966)	0.743 (0.671–0.806)	0.709(0.417–0.815)	0.958 (0.749–1.000)
VP model	0.941 (0.860–1.000)	0.886 (0.829–0.929)	0.874 (0.000–0.974)	0.958 (0.750–1.000)
Radiomics model	0.941 (0.860–1.000)	0.886 (0.829–0.929)	0.874 (0.000–0.974)	0.958 (0.750–1.000)
COMB model	0.980 (0.961–1.000)	0.943 (0.897–0.972)	0.947 (0.815–0.994)	0.917 (0.792–1.000)

Abbreviations: AP, arterial phase; VP, venous phase; COMB, combined.

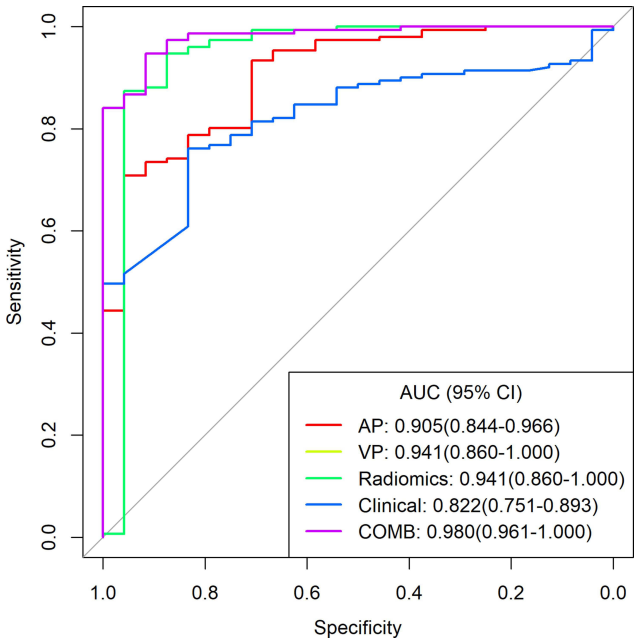

Figure 3 ROC curve of each diagnostic model.
Abbreviations: AP, arterial phase multivariate regression model; VP, venous phase multivariate regression model; Radiomics, arterial phase combined with venous phase omics model; Clinical, clinical feature model; COMB, radiomics combined with clinical feature comprehensive model.

features to establish a COMB model, which could intuitively reflect the overall characteristics of the lesion, and has high sensitivity (0.947, 95% CI: 0.815–0.994) and specificity (0.917, 95% CI: 0.792–1.000). Next, the radiomics features were analyzed, and the features were selected through the feature selection procedure. Ultimately, the radiomics model is the same as the VP model. Herein, we established five models: AP multivariate regression model, VP multivariate regression model, AP combined with VP omics model, clinical feature model, and radiomics combined with clinical feature comprehensive model. The results showed that the AUC (0.980; 95% CI: 0.961–1.000) of the clinical feature combined with the radiomics features comprehensive model was significantly higher than that of the AP multivariate regression model (P = 0.004) and the clinical feature model (P < 0.001), and the differential diagnosis efficacy was optimal. The AUC of the AP combined with the VP radiomics model was consistent with the value of the VP radiomics model (0.941; 95% CI: 0.860–1.000). Moreover, the AUC of the VP radiomics model was greater than that of the AP group, and although the AUC between the two comparisons was not statistically significant, the sensitivity and accuracy of the model were higher than those of the AP model, indicating that the diagnostic performance of the VP image extraction was better than that of the AP model. The radiomics feature reflects the pathological changes of the lesion, the heterogeneity of the image, and the diagnosis of the characteristics of the lesion. The pathological characteristics of PC are mainly cancer cells, interstitial astrocytes, and interstitial fibrosis. The fibrosis produced by the interstitial reaction of the lesion prevented the penetration of the contrast agent; hence, PC appeared at a low density in each phase of the enhanced scan. The pathological features of pancreatitis were mainly inflammatory cell infiltration and fibrous tissue hyperplasia. The degree of enhancement was similar to fibrous tissue, with mild enhancement in the AP and delayed enhancement in the venous and delayed phases.[22] Although both PC and FP were low density in AP, the performance of the venous and the delayed phase was helpful in distinguishing these cancers. Therefore, the radiomics features of VP are more valuable for diagnosis than the AP. Zhang et al[20] analyzed the radiomics features of PC and FP in plain CT, AP, and VP. These showed that the discrimination of radiomics analysis and prediction model of plain CT was the best. The AUC of the analysis model of AP (0.801) was higher than the VP (0.769), which was different from this study and could be related to other factors, such as tumor heterogeneity, inconsistent geographic regions of the cases, and the difference in the scanning machine and scan parameters. This study did not include the plain CT, but the AUC, sensitivity, and

Table 3 DeLong Test for Pairwise Comparison of AUC of Each Model

Predictive Model	*P*	Predictive Model	*P*
AP model vs VP model	0.246	VP model vs Radiomics model	1
AP model vs Radiomics model	0.246	VP model vs Clinical model	0.037
AP model vs Clinical model	0.071	VP model vs COMB model	0.262
AP model vs COMB model	0.004	Radiomics model vs Clinical model	0.037
Clinical model vs COMB model	<0.001	Radiomics model vs COMB model	0.262

Abbreviations: AP, arterial phase; VP, venous phase; COMB, combined.

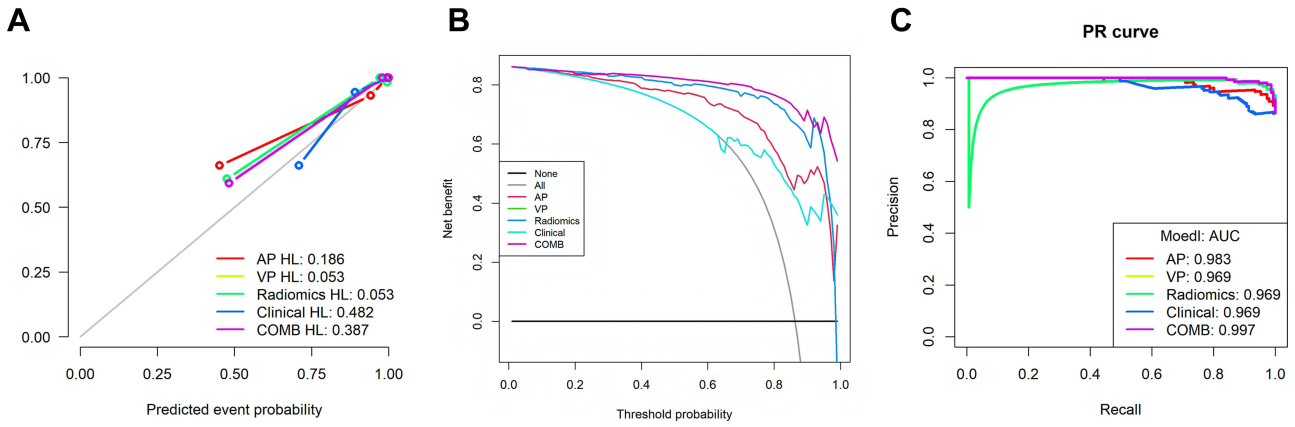

Figure 4 (**A**) Calibration curve of each model. (**B**) Decision curve of each model. (**C**) Precision recall curve of different models.
Abbreviations: AP HL, arterial phase multivariate regression model; VP HL, venous phase multivariate regression model; Radiomics HL, arterial phase combined with venous phase omics model; Clinical HL, clinical feature model; COMB HL, radiomics combined with clinical feature comprehensive model; AP, arterial phase multivariate regression model; VP, venous phase multivariate regression model; Radiomics, arterial phase combined with venous phase omics model; Clinical, clinical feature model; COMB, radiomics combined with clinical feature comprehensive model; AP, arterial phase multivariate regression model; VP, venous phase multivariate regression model; Radiomics, arterial phase combined with venous phase omics model; Clinical, clinical feature model; COMB, radiomics combined with clinical feature comprehensive model.

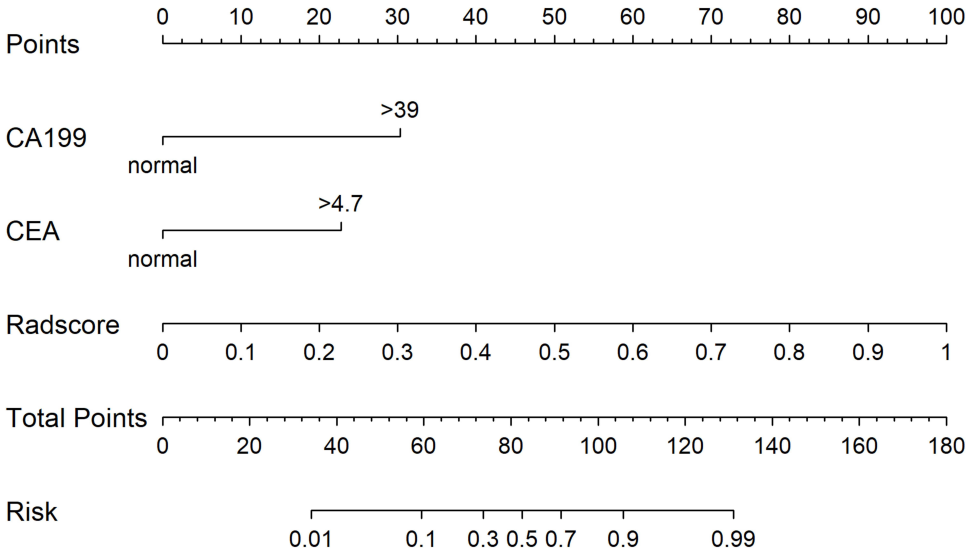

Figure 5 Nomogram established based on CA199, CEA, and imaging radiomics scores.

specificity of the AP and VP were higher, while the effectiveness was better than their results.

Tumor markers of PC have a guiding significance for early diagnosis and prognosis. CA19-9 and CEA are widely used and validated markers in PC.[23] However, CA19-9 is the only biomarker recommended for clinical use by the National Comprehensive Cancer Network (NCCN) guidelines for pancreatic cancer,[24] with 80% sensitivity and 80–90% specificity.[25] The optimal cutoff values for predicting advanced PC were 7.0 ng/mL for CEA and 305.0 U/mL for CA19-9. Although both tumor markers are independent predictors of advanced PC, CEA is a more robust predictor of advanced PC than CA19-9, resulting in positive predictive values of 83.3%, 73.6%, and 91.4% for CEA, CA19-9, and combination, respectively.[26] Strikingly, the combination of CA19-9 and CEA improves the specificity of diagnosing PC by 84%.[27] In addition, under certain inflammatory conditions, CA19-9 may also be upregulated. In this study, the levels of CA19-9 and CEA in patients with PC were significantly higher than those in patients with chronic pancreatitis, which is consistent with the previous findings.[28] The AUC value of the clinical feature model was 0.822 (95% CI: 0.751–0.893), and the AUC value of a single clinical

feature model was lower than any differential diagnosis model. Therefore, the combination of multiple indicators could improve the accuracy of diagnosis.

Surgical pathology is the gold standard for the diagnosis of PC and mass pancreatitis; however, some patients cannot be operated on because the lesion invades the surrounding blood vessels and nerves or has metastasized. The nomogram established by this study combined with CA19-9, CEA, and imaging radiomics scores is a non-invasive predictive tool that can analyze the overall characteristics of the lesion without being restricted by the location and size of the lesion, improving the accuracy of diagnosis while reducing patient trauma with optimal compliance.

Nevertheless, the present study has some limitations: 1) Only a small cohort of patients, especially the cases of mass pancreatitis and AIP, the differential diagnosis of mass pancreatitis, AIP, and PC was studied, and we failed to verify the prediction model. 2) The clinical data of some patients were missed, and the clinical data regarding amylase and antinuclear antibodies were not analyzed. 3) When delineating the ROI, some pancreatic cancer lesions had unclear borders surrounding the splenic artery, involving the spleen, and had an unclear boundary with adjacent tissues, reducing the accuracy of lesion delineation. 4) In this multicenter study, the scanning parameters and reorganization methods were different, and a unified standard was not determined. Thus, a multicenter program to collect FPs, localized AIP, and patients with PC and conduct clinical tests on large sample size is essential for external validation differential diagnosis model.

In conclusion, the COMB model, which combined clinical information and radiomics features based on enhanced VP CT, has the potential to be used to distinguish between pancreatic cancer and chronic pancreatitis.

Funding

This work was supported by the Project of Science and Technology Department of Hebei Province (192777131D); The Key Scientific research fund of Affiliated Hospital of Hebei University (2019Z009); The outstanding youth scientific research and innovation team of the Hebei University.

Disclosure

The authors report no conflicts of interest in this work.

References

1. Goral V. Pancreatic Cancer: Pathogenesis and Diagnosis. *Asian Pac J Cancer Prev*. 2015;16(14):5619-5624.
2. McGuigan A, Kelly P, Turkington RC, et al. Pancreatic cancer: a review of clinical diagnosis, epidemiology, treatment and outcomes. *World J Gastroenterol*. 2018;24(43):4846–4861.
3. Zhao Z, Liu W. Pancreatic cancer: a review of risk factors, diagnosis, and treatment. *Technol Cancer Res Treat*. 2020;19:15 33033820962117.
4. Pancreatic Cancer Committee of Chinese Anticancer Association. [Comprehensive guidelines for the diagnosis and treatment of pancreatic cancer (2020 version)]. *Chin J Surg*. 2021;59(2):81–100. Chinese.
5. Puckett Y, Garfield K. Pancreatic Cancer. 2021. In: *StatPearls [Internet]*. Treasure Island (FL): StatPearls Publishing; 2021.
6. Ren S, Chen X, Cui W, et al. Differentiation of chronic mass-forming pancreatitis from pancreatic ductal adenocarcinoma using contrast-enhanced computed tomography. *Cancer Manag Res*. 2019;20(11):7857–7866.
7. Okazaki K, Uchida K. Current perspectives on autoimmune pancreatitis and IgG4-related disease. *Proc Jpn Acad Ser B Phys Biol Sci*. 2018;94(10):412–427.
8. Dutta AK, Chacko A. Head mass in chronic pancreatitis: inflammatory or malignant. *World J Gastrointest Endosc*. 2015;7(3):258–264.
9. Dohan A, Gallix B, Guiu B, et al. Early evaluation using a radiomic signature of unresectable hepatic metastases to predict outcome in patients with colorectal cancer treated with FOLFIRI and bevacizumab. *Gut*. 2020;69(3):531–539.
10. Huang Z, Li M, He D, et al. Two-dimensional texture analysis based on CT images to differentiate pancreatic lymphoma and pancreatic adenocarcinoma: a preliminary study. *Acad Radiol*. 2019;26(8):e189–e195.
11. Li X, Zhu H, Qian X, et al. MRI Texture analysis for differentiating nonfunctional pancreatic neuroendocrine neoplasms from solid pseudopapillary neoplasms of the pancreas. *Acad Radiol*. 2020;27 (6):815–823.
12. Guo C, Zhuge X, Wang Z, et al. Textural analysis on contrast-enhanced CT in pancreatic neuroendocrine neoplasms: association with WHO grade. *Abdom Radiol (NY)*. 2019;44(2):576–585.
13. Yang J, Guo X, Zhang H, et al. Differential diagnosis of pancreatic serous cystadenoma and mucinous cystadenoma: utility of textural features in combination with morphological characteristics. *BMC Cancer*. 2019;19(1):1223.
14. Hanania AN, Bantis LE, Feng Z, et al. Quantitative imaging to evaluate malignant potential of IPMNs. *Oncotarget*. 2016;7 (52):85776–85784.
15. van Griethuysen JJM, Fedorov A, Parmar C, et al. Computational radiomics system to decode the radiographic phenotype. *Cancer Res*. 2017;77(21):e104–e107.
16. Sandrasegaran K, Lin Y, Asare-Sawiri M, et al. CT texture analysis of pancreatic cancer. *Eur Radiol*. 2019;29(3):1067–1073.
17. Ciaravino V, Cardobi N, DE Robertis R, et al. CT texture analysis of ductal adenocarcinoma downstaged after chemotherapy. *Anticancer Res*. 2018;38(8):4889–4895.
18. Cozzi L, Comito T, Fogliata A, et al. Computed tomography based radiomic signature as predictive of survival and local control after stereotactic body radiation therapy in pancreatic carcinoma. *PLoS One*. 2019;14(1):e0210758.
19. Ren S, Zhao R, Zhang J, et al. Diagnostic accuracy of unenhanced CT texture analysis to differentiate mass-forming pancreatitis from pancreatic ductal adenocarcinoma. *Abdom Radiol (NY)*. 2020;45 (5):1524–1533.
20. Zhang JJ, Li QZ, Wang JH, et al. Contrast-enhanced CT and texture analysis of mass-forming pancreatitis and cancer in the pancreatic head. *Zhonghua Yi Xue Za Zhi*. 2019;99(33):2575–2580. Chinese.

21. Zhang Y, Cheng C, Liu Z, et al. Radiomics analysis for the differentiation of autoimmune pancreatitis and pancreatic ductal adenocarcinoma in 18 F-FDG PET/CT. *Med Phys*. 2019;46(10):4520–4530.
22. Liu Y, Wang M, Ji R, Cang L, Gao F, Shi Y. Differentiation of pancreatic ductal adenocarcinoma from inflammatory mass: added value of magnetic resonance elastography. *Clin Radiol*. 2018;73(10):865–872.
23. Huang Z, Liu F. Diagnostic value of serum carbohydrate antigen 19-9 in pancreatic cancer: a meta-analysis. *Tumour Bio*. 2014;35(8):7459–7465.
24. Song JY, Chen MQ, Guo JH, et al. Combined pretreatment serum CA19-9 and neutrophil-to-lymphocyte ratio as a potential prognostic factor in metastatic pancreatic cancer patients. *Medicine (Baltimore)*. 2018;97(4):e9707.
25. Barhli A, Cros J, Bartholin L, et al. Prognostic stratification of resected pancreatic ductal adenocarcinoma: past, present, and future. *Dig Liver Dis*. 2018;50(10):979–990.
26. van Manen L, Groen JV, Putter H, et al. Elevated CEA and CA19-9 serum levels independently predict advanced pancreatic cancer at diagnosis. *Biomarkers*. 2020;25(2):186–193.
27. Kamisawa T, Wood LD, Itoi T, Takaori K. Pancreatic cancer. *Lancet*. 2016;388(10039):73–85.
28. Mayerle J, Kalthoff H, Reszka R, et al. Metabolic biomarker signature to differentiate pancreatic ductal adenocarcinoma from chronic pancreatitis. *Gut*. 2018;67(1):128–137.